tvst

Article

Risk Assessment of Aerosol Generation During Vitreoretinal Surgery Using High Speed Imaging Amidst the COVID-19 Pandemic

Chaitra Jayadev[1], Thirumalesh Mochi Basavaraj[1], Khushboo Pandey[2], Roven Pinto[2], Shashi Prabha Pandey[2], Saptarshi Basu[2], Abhijit Sinha Roy[3], and Rohit Shetty[1]

[1] Vitreoretina Department, Narayana Nethralaya Eye Institute, Bangalore, India
[2] Department of Mechanical Engineering, Indian Institute of Science, Bangalore, India
[3] Imaging, Biomechanics and Mathematical Modeling solutions, Narayana Nethralaya Foundation, Bangalore, India

Correspondence: Chaitra Jayadev, Department of Vitreoretina, Narayana Nethralaya Eye Institute, 121/C, Chord Road, 1 "R" Block, Rajajinagar, Bangalore 560010, Karnataka, India.
e-mail: drchaitra@hotmail.com

Received: April 20, 2021
Accepted: September 13, 2021
Published: October 14, 2021

Keywords: aerosols; coronavirus disease 2019 (COVID-19); droplets; high speed imaging; lensectomy; severe acute respiratory syndrome-coronavirus 2 (SARS-CoV-2); vitrectomy

Citation: Jayadev C, Mochi Basavaraj T, Pandey K, Pinto R, Pandey SP, Basu S, Roy AS, Shetty R. Risk assessment of aerosol generation during vitreoretinal surgery using high speed imaging amidst the COVID-19 pandemic. Transl Vis Sci Technol. 2021;10(12):17, https://doi.org/10.1167/tvst.10.12.17

Purpose: The purpose of this study was to discuss the propensity of aerosol and droplet generation during vitreoretinal surgery using high speed imaging amidst the coronavirus disease 2019 (COVID-19) pandemic.

Methods: In an experimental set up, various steps of vitreoretinal surgery were performed on enucleated goat eyes. The main outcome measures were visualization, quantification of size, and calculation of aerosol spread.

Results: During intravitreal injection, insertion of cannulas, lensectomy, and vitrectomy with both 23 and 25-gauge instruments, with either valved or nonvalved cannulas, aerosols were not visualized which was confirmed on imaging. Although there was no aerosol generation during active fluid air exchange (FAE), there was bubbling and aerosol generation at the exit port of the handle during passive FAE. Under higher air pressure, with reused valved and fresh nonvalved cannulas, aerosol generation showed a trajectory 0.4 to 0.67 m with droplet size of 200 microns. Whereas removing cannulas or suturing under active air infusion (35 mm Hg and above) aerosols were noted.

Conclusions: Based on the above experiments, we can formulate guidelines for safe vitrectomy during COVID-19. Some recommendations include the use of valved cannulas, avoiding passive FAE or to direct the exit port away from the surgeon and assistant, and to maintain the air pressure less than or equal to 30 mm Hg.

Translational Relevance: In the setting of the COVID-19 pandemic, the risk from virus laden aerosols, as determined using an experimental setup, appears to be low for commonly performed vitreoretinal surgical procedures.

Introduction

Severe acute respiratory syndrome coronavirus 2 (SARS-CoV-2) infection has been declared as a global pandemic by the World Health Organization since March 2020 and, as of late February 2021, 112,832,423 people have been infected worldwide, with over 2,500,308 having succumbed to the disease.[1,2] The SARS-CoV-2 viral infection is caused by the novel coronavirus and airborne transmission can occur via large droplets over short distances or via aerosols (smaller droplets) over large distances.[3,4] These viral laden droplets and aerosols are generated from breathing, coughing, and sneezing, and, in the healthcare environment, from aerosol generating procedures.[5,6] A cause for concern for the medical community is that surgical procedures are established as a risk factor after a series of surgeons tested positive for coronavirus disease 2019 (COVID-19) in China.[7] Likewise,

various surgical procedures performed by ophthalmologists can potentially generate aerosols containing the virus as it has been isolated from the conjunctiva and tears.[8–10]

Aerosol and droplet generating medical procedures or "surgeries with high speed devices" release particles as small (<20 microns) and large droplets (>20 microns).[11] The vitrectomy hand piece routinely used delivers between 5000 and 10000 cuts per minute and the mechanical vibration can cause the aerosol generation.[12] Other vitreoretinal surgical techniques, such as active or passive fluid-air exchange (FAE), could also generate droplets or aerosol. Although aerosol generation has been confirmed in some procedures,[13–15] ambiguity exists on whether they occur during vitreoretinal surgery. Hence, we aimed to determine the same by using high speed imaging.[16,17] This is a widely used imaging technique to study aerosols.[18] It uses a strobe light source, such as a pulsed laser or light emitting diode (LED), to capture the dark outline of fast-moving objects using a sufficiently fast shutter for a short exposure time.

Methodology

This experimental study was approved by the institutional research and ethics committee of Narayana Nethralaya Eye Institute, Bangalore, India, and conducted in accordance with the tenets of the Declaration of Helsinki. This approval was secured for the part of the study involving the use of animal tissue. Although it would have been ideal to do the experiments on cadaveric human eyeballs, we could not retrieve any due to the guidelines laid down by the Global Eye Bank Association and Eye Bank Association of India, which prohibited retrieval during the ongoing pandemic.[19,20] Hence, eyes of goats killed as part of routine commercial food production were utilized, which are easily available in our country. The study was performed in collaboration with scientists from the Indian Institute of Science, Bangalore, India.

Freshly enucleated goats' eyes were carefully inspected for uniformity and clarity of the ocular surface. The prepared eyes were mounted on a mannequin head to expose the cornea and sclera for surgical maneuvering (Fig. 1A). The Alcon Constellation Vision System LXT (Alcon, Fort Worth, TX, USA), part of a wet laboratory for training of residents, was used for the experiments. Other instruments used were dual-pneumatic, high speed 23- and 25-gauge cutters; 23- and 25-gauge valved, nonvalved, new, and used trocars and cannulas; and 20-guage microvitreoretinal (MVR) blade (Alcon). The different

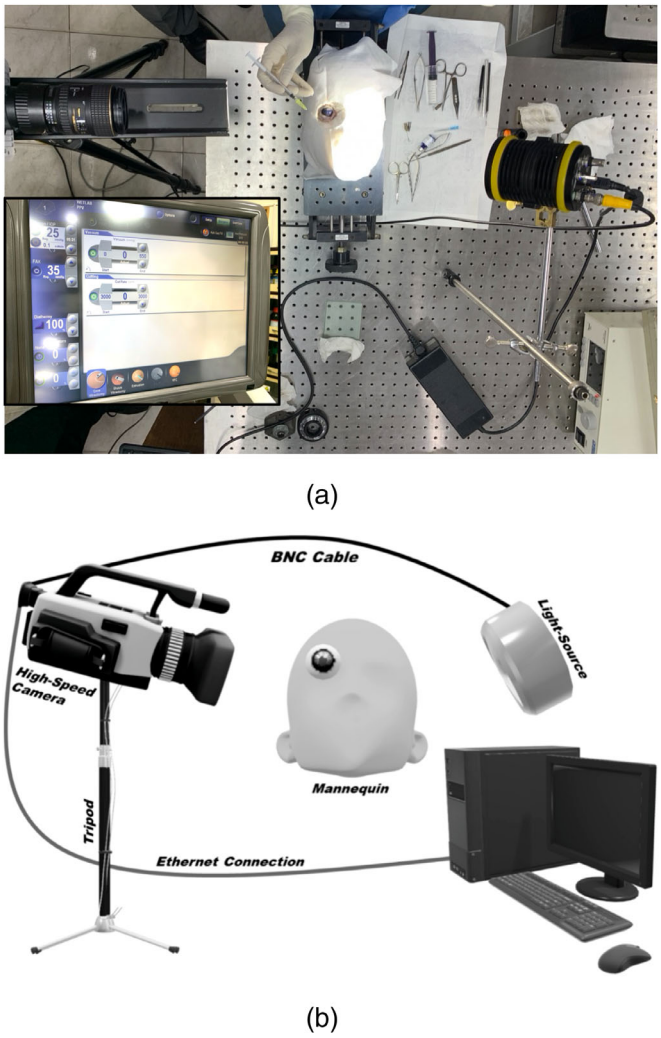

(a)

(b)

Figure 1. (**A**) Experimental set up for the vitreoretinal surgical procedures on animal eyes. (**B**) Experimental set up for high speed imaging.

steps of surgery for which aerosol generation was studied included the following:

1. Lensectomy – an infusion cannula (23- and 25-gauge valved/nonvalved) was placed 3.5 mm from the limbus; another cannula was placed 3 clock hours from the infusion cannula through which the lensectomy was done. Settings used were a cut rate of 3000, vacuum of 650 mm Hg, and infusion pressure of 25 mm Hg.
2. Vitrectomy – post lensectomy, vitrectomy was done using the same cannula. Settings used were a cut rate of 5000, vacuum of 650 mm Hg, and infusion pressure of 25 mm Hg.
3. Active FAE – using the suction mode of the cutter with an air pressure of 35 and 60 mm Hg.
4. Passive FAE – using the Charles flute needle and handle with an air pressure of 35 and 60 mm Hg.

5. Suturing – the 23-gauge scleral ports were sutured using 7-0 vicryl suture material.
6. 20-guage MVR scleral entry and exit – 3.5 mm from the limbus.
7. Intravitreal injections – a 30-gauge needle was used to inject fluid into the vitreous cavity 3.5 mm from the limbus.

The experimental setup used for the aerosol visualization is presented in Figure 1B. Droplet generation and trajectory was visualized using a high speed Photron SA5 camera coupled with a combination of macro-lens (Tokina 100 mm) and a 36 mm extension tube at 5000 fps (1024 × 1024 pixel resolution and 0.2 millisecond temporal resolution). The region of interest (ROI) was illuminated using a strobe lamp (Veritas 120 E LED Constellation) and the high speed imaging was done at a spatial resolution of 0.05 mm/pixel. Droplet size distribution and trajectories were isolated using two sets of in-house image processing algorithms in the ImageJ software. Using background subtraction, extraneous objects were removed from the ROI thereby segregating the droplets. Otsu thresholding was used for the image binarization.[21] Further, using particle analysis, droplet shape descriptors were evaluated from the binary images. The two-dimensional (2D) particle tracking technique of the MosaicSuite plugin of the ImageJ Software was utilized to evaluate droplet ejection velocity and predict its horizontal displacement (Video 1).[22]

Droplet Displacement

Droplet displacements are governed by the smaller of the evaporation or settling timescales. For droplets as small as 50 µm, the horizontal displacement is governed by their evaporation time ($t_{evaporation} \sim 9$ seconds) as compared to the bigger droplets where the settling timescale is more important. Hence for droplets of 50 µm diameter, horizontal displacement is approximately given as:

$$x = u_{air} t_{evaporation}$$

x value from the above calculation was found approximately 5.4 meters. Next, the total distance travelled (x) by the droplets (>50 µm) is calculated iteratively through computation using the following relations:

$$\frac{dx}{dt} = u_{droplet}$$

$$\frac{du_{droplet}}{dt} = \frac{4.5\mu_{air}\left(u_{air} - u_{droplet}\right)}{r_{droplet}^2 \rho_{droplet}}$$

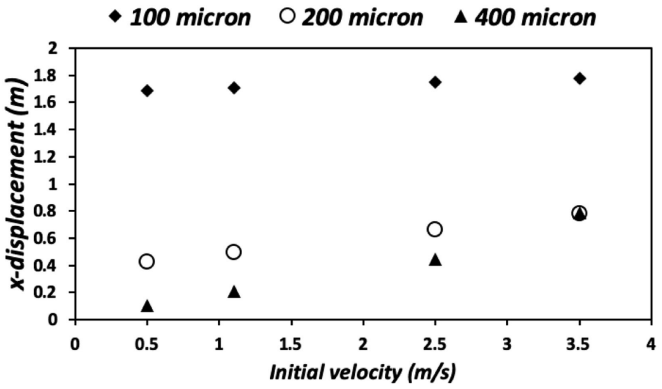

Figure 2. Variation in horizontal displacement with initial velocity for different droplet sizes.

Here, $u_{droplet}$ is the velocity of the droplet, u_{air} represents the surrounding convection velocity (taken as 0.6 m/s), $r_{droplet}$ is the droplet radius, t is time, μ_{air} is the viscosity of the surrounding air, and $\rho_{droplet}$ is the liquid droplet density. The droplet initial velocities were found to be in the range of 0.35 m/sec to 3.5 m/sec. Hence, for horizontal displacement calculations, these values are taken as the initial parameters along with the droplet diameter as shown in Figure 2.

Results

Three freshly enucleated goat eyes were used for the experiments, one each for the 23-guage and 25-guage procedures, whereas the third was used for the rest. All experiments were performed by a single vitreoretinal surgeon to reduce the variability in technique. Aerosol generation for each of the experiments had to be captured within 1 second at 5000 fps, and we repeated the procedures (ranging from 1–5 times) until we were able to capture the same. If aerosols were not imaged even after the fifth attempt, we concluded that there were no aerosols generated from that particular procedure. Each attempt at imaging was done from different angles so as to not miss imaging any of the generated aerosols. The pathway of droplet generation is bubble formation and its breakup. Continuous bubble expansion results in thinning of the liquid film (the bubble surface). Consequently, this layer shears off and the bubble bursts, thereby resulting in liquid ligaments. These ligaments further elongate and atomize to form smaller droplets or aerosols.

While performing intravitreal injections, insertion of cannulas (both 23- and 25-gauge and valved and nonvalved), lensectomy and vitrectomy with both 23- and 25-gauge instruments, with either valved or nonvalved cannulas and instrument exchange, we did not

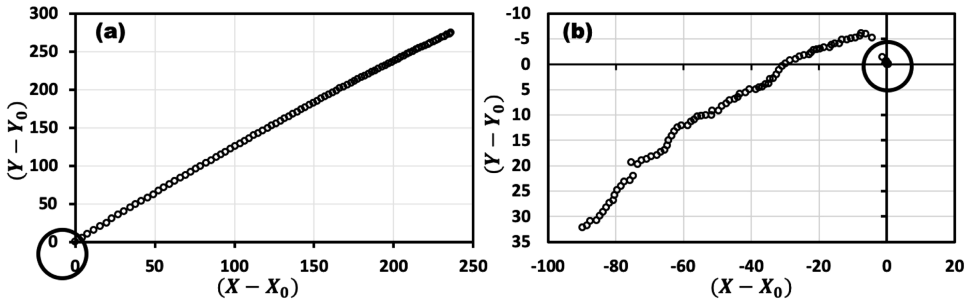

Figure 3. Droplet trajectory in a (X, Y) coordinate system. (**A**) Droplet approximately 150 µm, and (**B**) droplet approximately 800 µm. The *black circle* shows the points of origin, and X_0 and Y_0 is the initial position of the droplet.

find any aerosol generation, which was confirmed on high speed imaging. During the insertion and removal of a 20-guage MVR blade, there was fluid flow but no aerosols. Although there was no aerosol generation during active FAE while performing passive FAE using a Charles flute needle and handle, there was bubbling and aerosol generation at the exit port of the handle under higher air pressures.

Those procedures in which aerosols were visualized are further elucidated below:

23-guage valved under 60 mm Hg air pressure - During this procedure, droplets of sizes ranging between approximately 60 and 800 µm were observed. Ejection velocity for smaller droplets was approximately 0.1 to 1.0 m/sec whereas bigger droplets (approximately 800 µm) exhibited a velocity of approximately 0.009 m/sec. The trajectory of the smaller droplets were straight (Fig. 3A) whereas for bigger droplets (approximately 800 µm) it was parabolic (Fig. 3B).

25-guage valved under 60 mm Hg air pressure - During this procedure, droplets of sizes ranging between approximately 150 and 300 µm with an ejection velocity of approximately 0.35 to 1.0 m/sec were observed due to bubble break-up, as shown in Figure 4.

25-guage valved under 35 mm Hg air pressure - During this procedure, droplets of sizes ranging between approximately 100 and 300 µm with an ejection velocity of approximately 0.4 to 3.5 m/sec were observed post bubble rupture (Fig. 5).

25-guage valved cannula removal and suturing under 35 mm Hg air pressure - Droplets sized approximately 100 µm with an ejection velocity of approximately 0.45 to 2.2 m/sec were generated via bubble breakup and ligament formation.

Passive FAE with 35 mm Hg air pressure - Droplets sized approximately 300 to 800 µm were seen with an ejection velocity approximately 0.45 to 2.2 m/sec for smaller droplets and approximately 0.04 m/sec for bigger droplets (approximately 800 µm). These droplets were generated via bubble breakup and ligameet formation, as shown in Figure 6.

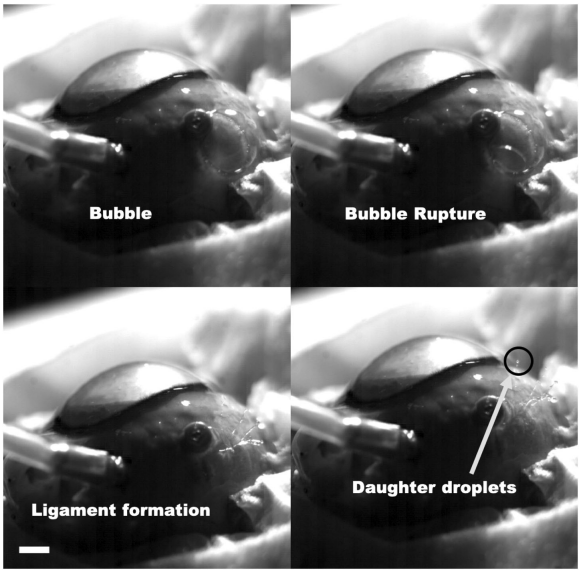

Figure 4. High speed snapshots of bubble undergoing rupture and generating droplets. Scale bar represents 2.5 mm.

We saw significant aerosols, even with valved cannulas, irrespective of the gauge when the air pressure was 35 mm Hg or more. We then gradually reduced the pressure and noted that aerosols were not observed in any of the procedures when the air pressure was 30 mm Hg or less.

Discussion

Ophthalmologists are likely to be at high risk of contracting COVID-19 due to aerosol generating procedures, both in the outpatient department and operating theatre. For the protection of eye surgeons

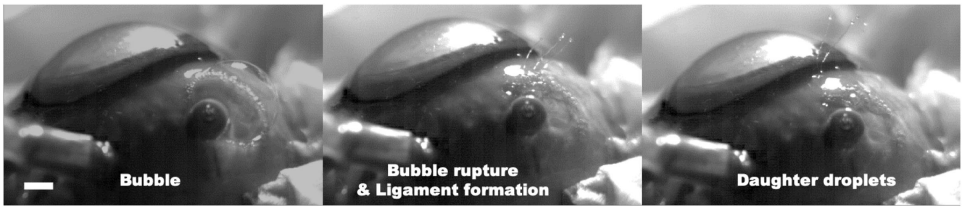

Figure 5. Formation of daughter droplets due to bubble break during passive fluid air exchange. Scale bar represents 2.5 mm.

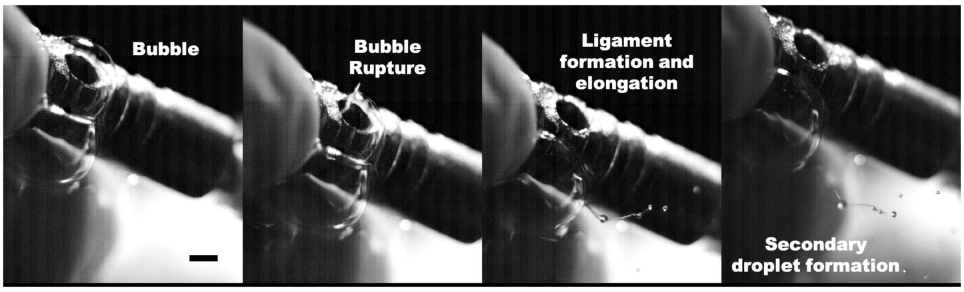

Figure 6. Secondary droplet formation during passive fluid air exchange. Scale bar represents 2.5 mm.

during this pandemic, it is not only essential to recognize which procedures are aerosolizing, but also to determine their risk potential. Whereas coughing and sneezing results in larger droplets, the risk of inhaling potentially smaller SARS-CoV-2 infected aerosols should not be neglected when performing procedures. With anecdotal reports on viral load in the tears and conjunctiva, the consequences could be serious. Hence, an effective risk assessment of common steps during vitreoretinal surgery can help understand the risk of transmission to health care professionals.[17] Because droplets in the size range of 0.05 to 500 µm contribute to the spread of airborne diseases, it was important to ascertain the size and spread of aerosols during surgical maneuvers.[23]

A high-resolution camera and high-speed imaging can capture particle sizes as small as 50 µm. Although imaging techniques like schlieren and shadowgraphy offer better resolution and lower detection limit, high speed imaging is simpler to implement and efficient when done at high frame rate (5000 fps) and using a fast shutter speed (0.2 millisecond).[24] Hence, both the resolving power of the imaging system and the acquisition rate are critical to ensure better droplet detection. With custom camera settings and adequate illuminating light source, a resolution of approximately 0.05 mm/pixel was possible for this study. In the aerosol generating procedures of our experiments, the droplets size was predominantly in the range of approximately 100 to 200 µm. Based on the initial velocity, their horizontal displacement was evaluated (and the range of displacement was found to be approximately 0.4–1.8 m). Another important determinant of how far the aerosols can travel is the trajectory. For smaller droplets, it was straight and parabolic for the bigger droplets approximately 800 µm. This implies that the bigger droplets settle down faster as compared to the smaller ones.

Using high speed imaging and a simulated vitreoretinal surgery set up, we sought to determine if aerosols are generated. Our methodology differs from previous similar studies.[12,25,26] We used enucleated animal eyes to more accurately simulate the biomechanics of human tissue and high-speed imaging to detect the smallest of aerosols during vitrectomy. The cannulas were placed 3 to 4 mm from the limbus to ensure that there is no influence on aerosol generation. Disruption of the surface tension of the air–fluid interface at the sclera or ports by mechanical or pressurized airflow gives rise to aerosols. A lensectomy was done to allow better visibility of the vitreous cavity as we could not use a visualization system for the experimental set up. During insertion of different types and gauges of cannulas or while doing vitrectomy or lensectomy, there were no aerosols noted. Possible reasons are that the high-frequency back-and-forth motion of the guillotine blade does not dispense enough energy or the direction or diffusion of energy release may not disrupt the interface sufficiently, or any droplets or aerosols formed by the blade at the interface are immediately aspirated by the vacuum or prevented from escaping to the surface, as noted by the absence of aerosols when valved cannulas were used, as also elucidated by Liyanage et al.[26]

Because vitrectomy is done in a "closed chamber," it is also less likely to generate aerosols. Unless there is an air–fluid interface, such as during FAE, aerosol production is negligible. We did not notice aerosols at the beginning of FAE or after completion of the process due to the absence of an air–fluid interface as long as the air pressure was less than or equal to 30 mm Hg. However, when the air pressure exceeded 30 mm Hg, we noticed significant aerosols, even with valved cannulas, irrespective of the gauge. This risk is higher for passive FAE as no aerosol was noted during active FAE using the suction of the vitrector. We also saw higher aerosol generation in reused and nonvalved cannulas. Another important point to keep in mind is that once the vitrectomy is complete, the source of the aerosols could be either contaminated surface hemorrhage and/or sterile balanced salt solution.

Keeping the above in consideration we recommend the following:

- the use of new and valved cannulas
- to avoid passive FAE or to direct the exit port of the handle away from the surgeon and assistant
- to maintain air pressure at less than or equal to 30 mm Hg
- to stop active pressurized air infusion or clamp the air infusion tubing prior to removal of cannulas and suturing.

Our aim was to assess the risk of transmission of SARS-CoV-2 virus from infected patients to the operating surgeon during surgery. There are no reports so far of the coronavirus being detected in the aqueous or vitreous humor. However, with evidence of the virus being isolated from the ocular surface, it could pose a threat to vitreoretinal surgeons.[9] With the routine pre-operative povidone iodine preparation prior to any intraocular surgery and the virucidal activity of iodine, the presence of virus in the conjunctival sac is likely to be low.[27,28] Furthermore, the risk of disease transmission during surgery can be minimized if additional precautions, such as masks for the patients, use of betadine prior to the surgery, and the use of a protective shield between the surgical area and personnel when feasible.[29–31] Recent evidence suggests that medical masks and N95 respirators offer similar protection against COVID-19 in healthcare workers during non-aerosol-generating care.[32–33] Although there has been no trial so far on specifically preventing COVID-19, wearing N95 respirators can prevent 73 more clinical respiratory infections per 1000 healthcare workers compared to surgical masks.[34]

Aerosols emitted during breathing and typical speech average only 1 μm in diameter but, despite their small size, they are large enough to carry a variety of respiratory pathogens.[35] We were able to demonstrate the generation of aerosols with pathogen carrying potential, and the speed and distance travelled by them during vitrectomy procedures. It not only helps us to formulate guidelines on safe practice during this pandemic, but also guide us on remedial measures during the surgical procedure. Given the limitations of the available research and knowledge surrounding this topic and based on the findings of this study, we recommend vitreoretinal surgeons to be cautious. As the consequences of being infected with SARS-CoV-2 are significant, a careful balance between the potential harms of the procedure and adopting enhanced personal protective protocols is reasonable. The quantification of the aerosol generation, direction, and speed helps to take practical decisions in surgical techniques during the pandemic. Further research is needed to clarify the degree to which various personal protective equipment reduces the risk associated with each procedure during the COVID-19 pandemic.

Acknowledgments

Disclosure: **C. Jayadev,** None; **T. Mochi Basavaraj,** None; **K. Pandey,** None; **R. Pinto,** None; **S.P. Pandey,** None; **S. Basu,** None; **A.S. Roy,** None; **R. Shetty,** None

References

1. World Health Organization. WHO Director-General's opening remarks at the media briefing on COVID-19, https://www.who.int/dg/speeches/detail/who-director-general-s-opening-remarks-at-the-media-briefing-on-covid-19—11-march-2020. Accessed February 24, 2021.
2. Reported cases or deaths by Country Territory or conveyance, https://www.worldometers.info/coronavirus/. Accessed February 24, 2021.
3. Tellier R, Li Y, Cowling BJ, Tang JW. Recognition of aerosol transmission of infectious agents: a commentary. *BMC Infect Dis* 2019;19:101.
4. Jones RM, Brosseau LM. Aerosol transmission of infectious disease. *J Occup Environ Med*. 2015;57:501–508.
5. Rothan HA, Byrareddy SN. The epidemiology and pathogenesis of coronavirus disease (COVID-19) outbreak. *J Autoimmun*. 2020;109:102433.

6. Chandra A, Haynes R, Burdon M, et al. Personal protective equipment (PPE) for vitreoretinal surgery during COVID-19. *Eye (Lond)*. 2020;34(7):1196–1199.
7. Liu Z, Zhang Y, Wang X, Zhang D, et al. Recommendations for Surgery During the Novel Coronavirus (COVID-19) Epidemic. *Indian J Surg*, https://doi.org/10.1007/s12262-020-02173-3. Online ahead of print.
8. Lu CW, Liu XF, Jia ZF. 2019-nCoV transmission through the ocular surface must not be ignored. *Lancet*. 2020;395:e39.
9. Kumar K, Prakash AA, Gangasagara SB, et al. Presence of viral RNA of SARS-CoV-2 in conjunctival swab specimens of COVID-19 patients. *Indian J Ophthalmol*. 2020;68:1015–1017.
10. Seah IYJ, Anderson DE, Kang AEZ, et al. Assessing Viral Shedding and Infectivity of Tears in Coronavirus Disease 2019 (COVID-19) Patients. *Ophthalmology*. 2020;127(7):977–979.
11. Tellier R. Review of aerosol transmission of influenza A virus. *Emerg Infect Dis*. 2006;12:1657–1662.
12. Koshy ZR, Dickie D. Aerosol generation from high speed ophthalmic instrumentation and the risk of contamination from SARS COVID19. *Eye (Lond)*. 2020;4:1–2.
13. Mick P, Murphy R. Aerosol-generating otolaryngology procedures and the need for enhanced PPE during the COVID-19 pandemic: a literature review. Version 2. *J Otolaryngol Head Neck Surg*. 2020;49(1):29.
14. Khamar P, Shetty R, Balakrishnan N, et al. Aerosol and droplet creation during oscillatory motion of the microkeratome amidst COVID-19 and other infectious diseases. *J Cataract Refract Surg*, https://doi.org/10.1097/j.jcrs.0000000000000326. Epub ahead of print. PMID: 32675657.
15. Shetty N, Kaweri L, Khamar P, et al. Propensity and quantification of aerosol and droplet creation during phacoemulsification with high-speed shadowgraphy amidst COVID-19 pandemic. *J Cataract Refract Surg*, https://doi.org/10.1097/j.jcrs.0000000000000289. Epub ahead of print. PMID: 32649436.
16. Cackett P, Bennett H. Phacoemulsification and pars plana vitrectomy: no evidence of an increased risk of aerosol transmission. *Eye (Lond)*. 2020;35:1274.
17. Wong R, Banerjee PJ, Kumaran N. Part 2 model eye simulation: aerosol generating procedures in intraocular surgery. *Eye (Lond)*. 2021;35:1791–1792.
18. Castrejón-Pita JR, Castrejón-García R, Hutchings IM. High Speed Shadowgraphy for the Study of Liquid Drops. In: Klapp J, Medina A, Cros A, Vargas C, (eds). *Fluid Dynamics in Physics, Engineering and Environmental Applications. Environmental Science and Engineering (Environmental Engineering)*. Berlin, Heidelberg: Springer Inc.; 2013:121–137.
19. Sharma N, D'Souza S, Nathawat R, et al. All India Ophthalmological Society - Eye Bank Association of India consensus statement on guidelines for cornea and eyebanking during COVID-19 era. *Indian J Ophthalmol*. 2020;68(7):1258–1262.
20. http://www.gaeba.org/wp-content/uploads/2020/03/GAEBA-COVID19-Alert-25-March-2020.pdf. Accessed February 24, 2021.
21. Otsu N. A threshold selection method from gray-level histograms. *Automatica* 1975;11:23–27.
22. Sbalzarini IF, Koumoutsakos P. Feature point tracking and trajectory analysis for video imaging in cell biology. *J Struct Biol*. 2005;151(2):182–195.
23. Gralton J, Tovey E, McLaws ML, Rawlinson WD. The role of particle size in aerosolised pathogen transmission: a review. *J Infect* 2011;62:1–13.
24. Tang JW, Nicolle AD, Pantelic J, et al. Qualitative real-time schlieren and shadowgraph imaging of human exhaled airflows: an aid to aerosol infection control. *PLoS One*. 2011;6:e21392.
25. Wong R, Bannerjee P, Kumaran N. Aerosol generating procedures in intraocular surgery. *Eye (Lond)*, https://doi.org/10.1038/s41433-020-0997-7. Epub ahead of print. PMID: 32467634.
26. Liyanage S, Ramasamy P, Elhaddad O, et al. Assessing visible aerosol generation during vitrectomy in the era of Covid-19. *Eye (Lond)*. 2021;35:1187–1190.
27. Eggers M, Eickmann M, Zorn J. Rapid and effective virucidal activity of povidone-iodine against Middle East respiratory syndrome coronavirus (MERS-CoV) and modified vaccinia virus ankara (MVA) *Infect Dis Ther*. 2015;4:491–501.
28. Kariwa H, Fujii N, Takashima I. Inactivation of SARS coronavirus by means of povidone-iodine, physical conditions and chemical reagents. *Dermatology*. 2006;212(Suppl 1):119–123.
29. Darcy K, Elhaddad O, Achiron A, et al. Aerosol during phaco (cataract surgery). How to make cataract surgery safe during Covid-19. Accessed July 20, 2020, https://www.youtube.com/watch?v=8LGwI9LIYmU&feature=youtube.
30. Weber A, Willeke K, Marchioni R, et al. Aerosol penetration and leakage characteristics of masks used in the health care industry. *Am J Infect Control*. 1993;21(4):167–173.

31. Radonovich LJ, Simberkoff MS, Bessesen MT, et al. N95 Respirators vs Medical Masks for Preventing Influenza Among Health Care Personnel: A Randomized Clinical Trial. *JAMA*. 2019;322(9):824–833.
32. Smith JD, MacDougall CC, Johnstone J, et al. Effectiveness of N95 respirators versus surgical masks in protecting health care workers from acute respiratory infection: a systematic review and meta-analysis. *CMAJ*. 2016;188(8):567–574.
33. Bartoszko JJ, Farooqi MAM, Alhazzani W, Loeb M. Medical masks vs N95 respirators for preventing COVID-19 in healthcare workers: A systematic review and meta-analysis of randomized trials. *Influenza Other Respir Viruses*. 2020;14(4):365–373.
34. Iannone P, Castellini G, Coclite D, et al. The need of health policy perspective to protect Healthcare Workers during COVID-19 pandemic. A GRADE rapid review on the N95 respirators effectiveness. *PLoS One*. 2020;15(6):e0234025. Published 2020 Jun 3.
35. Asadi S, Wexler AS, Cappa CD, Barreda S, Bouvier NM, Ristenpart WD. Aerosol emission and superemission during human speech increase with voice loudness. *Sci Rep*. 2019;9(1):2348.

Supplementary Material

Supplementary Video 1. Droplet trajectories extracted from 2D particle tracking.